

# Evaluation the cardiopulmonary markers in cecal ligation and puncture-induced sepsis in Wistar rats

Tina Didari<sup>1</sup>, Shokoufeh Hassani<sup>1</sup>, Maryam Baeri<sup>1</sup>, Vida Kazemi<sup>2#</sup>, Mohammad Abdollahi<sup>1,3</sup>, Mojtaba Mojtahedzadeh<sup>1,4#</sup>

<sup>1</sup> Pharmaceutical Sciences Research Center (PSRC), The Institute of Pharmaceutical Sciences (TIPS), Tehran University of Medical Sciences, Tehran, Iran.

<sup>2</sup> Medicinal Plants Research Center, Faculty of Pharmacy, Tehran University of Medical Sciences, Tehran, Iran.

<sup>3</sup> Department of Toxicology and Pharmacology, School of Pharmacy, Tehran University of Medical Sciences, Tehran, Iran.

<sup>4</sup> Department of Clinical Pharmacy, School of Pharmacy, Tehran University of Medical Sciences, Tehran, Iran.

# Corresponding Authors:

Mojtaba Mojtahedzadeh (Email: Mojtahed@tums.ac.ir)

Dr.Vida Kazemi (E-mail: kazemi-V@razi.tums.ac.ir)

(Submitted: 29 July 2020 – Revised version received: 19 August 2020 – Accepted: 07 September 2020 – Published online: 30 October 2020)

## Abstract:

**Objective:** Sepsis is a clinical problem caused by host immune disability against pathogens. Rodent Cecal Ligation and Puncture (CLP) models mimic sepsis in humans. Gauges needle size in CLP is related to cytokine storm, inflammation, and organ failure. This study focus, for the first time, on precise and inexpensive biochemical markers to evaluate the difference of sepsis severity in the heart and lung tissues, one day after cecal ligation and puncture-induced sepsis with needle gauge 18 (G-18).

**Methods:** Twelve adult male Wistar rats were randomly allocated into two groups of six animals. These groups include; sham operation as the control group and underwent CLP procedure with G-18. All rats were sacrificed 24 hours after CLP. Then lungs and heart samples were collected for biochemical and histological assessment. Following the procedure, reactive oxygen species (ROS), Myeloperoxidase Activity (MPO), Tumor Necrosis Factor-Alpha (TNF- $\alpha$ ), High Mobility Group Box 1 (HMGB1), lactate generation, caspases (-3 and -9), gene expression of autophagy, cellular hypoxia, and pathological assessment of both tissues were measured.

**Results:** Increased level of ROS, MPO, pro-inflammatory cytokines, hyperlactatemia, caspases production, overexpression of hypoxia (PRKAA1 gene), and autophagy (MAP1LC3B gene) in the lungs were higher compared to heart 24 hours after the procedure. Moreover, hyperplasia of pneumocyte and inflammatory cells, and myocardial necrosis were found in the pathological assessment.

**Conclusion:** The purpose of study was to determine the severity of sepsis by means of cost-effective and precise inflammatory markers. Our findings demonstrated that injury-related indicators in lungs meaningfully increased compared to heart 24 hours after CLP.

**Keywords:** Sepsis, Cecal Ligation and Puncture (CLP), Inflammation, Oxidative stress, Needle gauge

## Introduction

Sepsis is a common cause of inpatient mortality in both genders and all age groups, particularly in the intensive care units of hospitals. Annually, more than 19 million people are affected by sepsis (with a mortality rate as high as 18%) worldwide.<sup>1,2</sup> In sepsis, the cause of death is generally multiorgan dysfunction syndrome (MODS). Despite the recent decrease in its mortality rate which can be attributed to the advancements in antibiotics and intensive care equipment, the incidence of sepsis is increasing worldwide.<sup>3</sup>

Sepsis-induced shock is associated with multiorgan failure and mortality rate of patients with sepsis. The most frequently affected organs by sepsis are those of the cardiovascular and respiratory systems.<sup>4</sup> Although the precise mechanisms of sepsis-induced cardiomyopathy are not yet fully elucidated, it suggested that severe inflammation, metabolism insufficiencies, and defective beta-adrenergic response may be involved in this process.<sup>3</sup> It is demonstrated that pulmonary complications of sepsis are due the cumulative effect of circulating cellular elements, soluble inflammatory mediators, and cytokines on the pulmonary tissues.<sup>5</sup>

Considering its high fatality rate, sepsis leaves little opportunity for clinical research in the field. Therefore, the CLP procedure (which is considered as the gold-standard model of human sepsis) provides the opportunity for an investigation into different aspects of this condition. During this procedure,

secretion of intestinal polymicrobial flora into the abdomen leads to development of systemic presentations very similar to those caused by sepsis in humans.<sup>6</sup>

CLP-induced damages (and sepsis in humans) stimulate the immune system, activate oxidative stress pathways, increase caspase levels (due to apoptosis), lead to the production of early and late proinflammatory cytokines such as TNF- $\alpha$  and HMGB1 and upregulation of autophagy and hypoxia-related genes.<sup>7</sup> Reactive oxygen species (ROS) are major signaling molecules involved in the oxidative stress response. In sepsis, the excessive accumulation of ROS impairs cellular homeostasis, and this leads to oxidative stress and mitochondrial dysfunction. This oxidative stress process, caspases activation, and hyperinflammation also promote autophagy, a defensive cytoprotective process for recycling waste organelles and other intracellular material following cellular damages.<sup>8</sup> Therefore, indicators of oxidative stress and autophagy processes have been widely used to investigate the intensity of sepsis induced through CLP procedure.<sup>9</sup> Similarly, measurement of the enzyme AMP-activated protein kinase (AMPK) is extensively applied for assessment of severity of sepsis.<sup>10</sup> This ROS elevation also promotes autophagy, a defensive cytoprotective process for recycling waste organelles and other intracellular material following cellular damages.<sup>8</sup> Consequently, autophagy proteins such as LC3B are considered most valuable

biomarkers for evaluation of cellular impairment.<sup>9</sup> Similarly, measurement of the enzyme AMPK and autophagy proteins are employed for assessment of molecular dysfunction.<sup>10</sup>

It is demonstrated that the size of the needle used in the CLP procedure can be influential in different septic outcomes such as mortality, cytokines concentrations, apoptosis, lactic acidosis, and autophagy. Previous studies has showed that G-18 induced MODS more efficiently compared to other gauge groups.<sup>6, 11, 12</sup>

There exist limited experiments on factors affecting MODS with G-18. The current study was designed and carried out with different views. Firstly, a period of 24 hours was chosen for investigation into the severity of sepsis in the cardiovascular and pulmonary systems. Doing this, we managed to minimize the duration of the study and reduce the costs involved in animals' care following the procedure. Moreover, in the current study, for the first time, we employed autophagy gene expression and cellular hemostasis indicators (along with simultaneous assessment of cellular hemostasis and measurement of primary and secondary inflammatory cytokines) for assessment of cytokine storm. Moreover, appropriate target tissues (pulmonary and cardiac) were chosen for investigation into sepsis induced through CLP procedure. Lastly, we employed low-cost, convenient, and precise laboratory tests for assessment of the extent of tissue damage (such as lactate, oxidative stress, and apoptosis).

## Material and methods

### Animals

Adult male Wistar rats 3–4 months old (250–300 g) were procured from the animal breeding house of the faculty of the pharmacy of TUMS. Animals were kept according to the animal standard care facility under controlled temperature (23 ± 10°C), 12 h light/dark cycle, 55± 10% humidity, and ad libitum feed. The protocol of the study was approved by the institutional ethical committee under code number IR.TUMS.VCR.REC.1396.2341.

### Reagents

For High mobility group box 1 (HMGB1) and TNF- $\alpha$ , ELISA kits were obtained from ZellBio GmbH (Ulm, Germany) and Diaclone (France), respectively. The lactate isolation kit was produced from ZellBio GmbH (Ulm, Germany). RNase solution, iScript cDNA synthesis kit, and propidium iodide were manufactured by Sigma-Aldrich GmbH (Munich, Germany). Other chemicals not specifically mentioned were all purchased from Sigma-Aldrich GmbH (Munich, Germany).

### Animal Groups

All male Wistar rats were randomly divided into the following three groups:

Sham or control group (which underwent the same operation without the CLP procedure) and CLP group with G-18 (which was operated with two punctures of G-18)

### The Procedure

Adult male Wistar rats first underwent CLP as described in detail elsewhere.<sup>11</sup> Rats were anesthetized with ketamine and xylazine. Then, the cecum was ligated with a 3.0 silk suture at its base right below the ileocecal valve, and two punctured using G-18. Next, the abdomen was closed using silk suture.

Following the operation, animals were hydrated through intravenous administration of an isotonic saline solution, returned to a cage in 24 hours.<sup>13</sup> According to previous research, sepsis induced 6 hours after CLP.<sup>11, 12</sup>

### Sample Collection

Twenty-four hours after CLP, the animals were sacrificed. Heart and lung tissues were harvested, then put into two parts for further histopathological and biochemical assessments.

## Assessment of Biochemical Variables

### ROS Assay

Tissue samples were all homogenized and centrifuged accordingly. Subsequently, they were stored in 75  $\mu$ L extraction buffer, mixed with 80  $\mu$ L of assay buffer, and kept for 30 min at 37 °C. Production of ROS was absorbed by 2', 7'-dichlorofluorescein diacetate (DCF-DA) as a fluorogenic reagent. Identification of the absorbance change of DCF-DA was identified using ELISA fluorometer (Biotec, Tecan U.S.) with maximum excitation (488 nm) and emission (529 nm) spectra for an hour.

### Myeloperoxidase (MPO) Activity

Briefly, tissue samples were homogenized in 50 mM potassium buffer (pH 6.0) containing 0.5% HTAB. Subsequently, the samples were centrifuged (30,000g, 15 min, 4 °C) and the supernatant was mixed with phosphate buffer (pH 6, 50 mM). Change of absorbance was recorded through spectrophotometric analysis at 460 nm 5 minutes later, as described in detail elsewhere.<sup>14</sup>

### Lactate Levels in Tissue Samples

According to the Manufacturer's protocol, lactate assay was performed for analysis of all samples. In short, tissue samples (100 mg) were homogenized in 8% perchloric acid and lactate level evaluated using a standard curve.

### Caspase-3 and -9 Activity

Colorimetric assays were utilized for measurement of the caspases-3 and -9 through specific identification of particular amino acid sequences. Briefly, the color changed and detected by spectrophotometry as setup by Rahimifard.<sup>15</sup>

### Assessment of Pro-inflammatory Cytokines (TNF- $\alpha$ and HMGB1)

The quantity of rat-specific TNF- $\alpha$  and HMGB1 in test samples were examined by a rat-specific ELISA kit. All test steps were performed according to the manufacturer's protocol.

### Gene Expression Evaluation

For real-time reverse transcription-polymerase chain reaction (RT-qPCR), 1  $\mu$ g of total RNA was reverse transcribed to cDNA using a Primescript RT reagent kit (TAKARA, Japan). RT-qPCR was performed using the Step one plus ABI system (Applied Biosystems). RT-qPCR was carried out under manufacturer's instruction.<sup>16</sup> The sequences of primers used for RT-qPCR are presented in Table 2.

### Histopathological Studies

The animals were euthanized 24 hours after the procedure, and heart and lung tissues were isolated and fixed in the 10%

neutral buffered formalin (NBF, pH 7.26) for 48 hours, and then were embedded in paraffin and stained with hematoxylin and eosin (H&E), then observed using a light microscope (Olympus BX51, Japan). Any suspected changes were recorded. 200 x (scale bar=100µm), 400 x (scale bar=20µm).

### Statistical Analysis

The results were presented as the mean ± standard error of the mean (SEM). One-way analysis of variance (ANOVA) and Tukey's multicomparison tests was applied with the degree of significance set at  $P < 0.05$ . Statistical analyses were performed using GraphPad Prism version 5 (GraphPad Software, La Jolla, CA, USA).

## Results

### ROS Generation

ROS levels were raised significantly in heart of CLP compared to the sham group ( $P < 0.01$ ). Moreover, ROS production in the lung was increased significantly in CLP compared to the sham group ( $P < 0.001$ ). A significant difference was not found between the lung and heart tissue of the CLP group (Table 1).

### Myeloperoxidase Activity

The result of MPO assay as neutrophil infiltration marker showed that a significant elevation in the heart ( $P < 0.01$ ) and lung ( $P < 0.001$ ) samples of the CLP group in comparison with related sham groups. Moreover, no significant differences were found between the heart and lung tissues of CLP groups (Table 1).

### Lactate Levels

Lactate production, a reliable marker of tissue hypoperfusion and hypoxia was increased in both heart ( $P < 0.01$ ) and lung ( $P < 0.001$ ) samples of CLP group, compared to related sham groups. Hyperlactatemia was significantly increased in the lung ( $P < 0.001$ ) compared to the heart sample of the CLP group (Table 1).

### Caspase 3 and Caspase 9

Caspases as cysteine proteases family activate during apoptosis. The result showed meaningfully hyperactivation of caspase-3 in the heart ( $P < 0.001$ ) and lung ( $P < 0.001$ ) specimens of CLP groups, compared to related sham groups. Also,

caspase-3 activity was increased in the lung compared to heart tissue in the CLP group ( $P < 0.05$ ).

Moreover, it found that caspase-9 significantly elevated in the heart ( $P < 0.001$ ) and lung ( $P < 0.001$ ) samples of CLP groups, compared to related sham groups. A significant increase of caspase-9 activity was observed in the lung compared to the heart tissue of the CLP group ( $P < 0.05$ ) (Table 1).

### Proinflammatory Cytokines

TNF- $\alpha$  which is an early modulator of inflammation during sepsis was found to be significantly increased in the heart and lung tissue of the CLP group ( $P < 0.001$ ) in comparison with the related sham groups. The levels of TNF- $\alpha$  in lung tissue were increased compared to the heart sample in the CLP group ( $P < 0.001$ ).

The amount of HMGB1, a late phase inflammatory biomarker, was significantly elevated in the heart and lung tissue of the CLP group ( $P < 0.001$ ) in comparison with the related sham groups. The levels of HMGB1 in lung tissue were increased compared to the heart sample in the CLP group ( $P < 0.001$ ) (Fig. 1).

### Real-Time Reverse Transcription-Polymerase Chain Reaction (RT-qPCR)

The mRNA expression level of the Prkaa1 gene (related gene to AMPK activity, as the stress protein) in the heart (1.77-fold) and lung sample (3.66-fold) was significantly increased in CLP group compared to the sham group. Also, the mRNA expression level of Prkaa1 was increased significantly in lung tissue compared to the heart specimens in the CLP group ( $P < 0.001$ ).

The mRNA expression level of the Map1lc3b gene (related gene to activation of LC3IIb, as an autophagy indicator) in the heart (4.38-fold) and lung samples (5.86-fold) was significantly elevated in CLP group compared to the sham group. The analysis of the mRNA expression level of Map1lc3b data showed that lung tissue has been significantly increased compared to the heart samples in the CLP group ( $P < 0.05$ ) (Fig. 2).

The abbreviations and primers of proteins used for real-time RT-qPCR listed in Table 2.

### Histopathological Analysis

All the samples were visualized by an independent reviewer. The results of each sample have reported that micrographs of the lung in the CLP group showed various degrees of lung

Table 1. Effect of gauge-18 on biochemical markers of lung and heart tissue, 24 hrs. after CLP.

Variables	Groups			
	Sham-Heart	CLP-Heart	Sham-Lung	CLP-Lung
ROS (u/mg protein)	0.66±0.05	1.21±0.08**	0.27±0.03	0.98±0.16***
MPO (unit/gr tissue)	77.83±3.64	112.64±7.44**	75.97±7.50	130.11±7.20***
Lactate levels (mmol/L)	2.90±0.07	4.18±0.12**	6.47±0.11	10.06±0.45*** ...
Caspase 3 (% of content)	83.04±1.85	117.60±1.45***	100.12±2.52	138.29±8.97*** .
Caspase 9 (% of content)	85.17±7.35	114.94±1.43***	83.18±3.10	132.77±2.35*** .

Results are expressed as mean ± SEM for six animals in each group. \*\*\*: significant difference from the related sham group at  $P < 0.001$ , \*\*: significant difference from the related sham group at  $P < 0.01$ , ...: significant difference from CLP-Heart group at  $P < 0.001$ , .: significant difference from CLP-Heart group at  $P < 0.05$ .

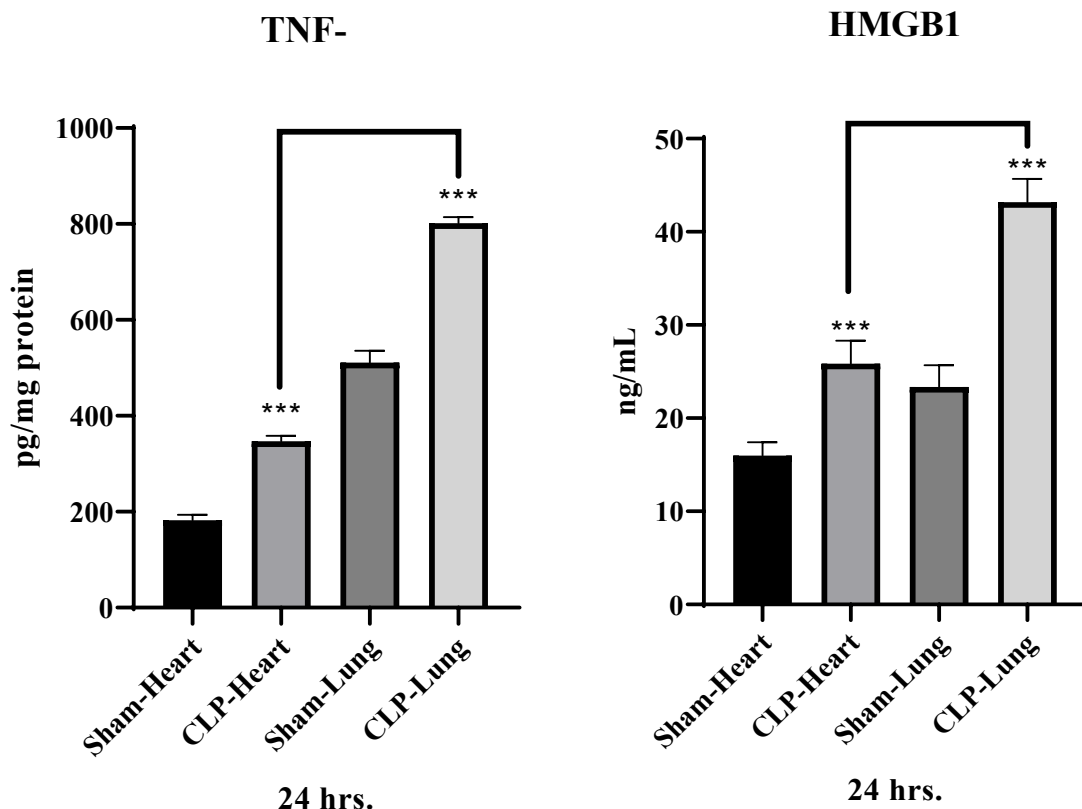


Fig. 1. Assessment of proinflammatory cytokines level in heart and lung injury, one day after CLP with gauge 18. Tumor Necrosis Factor- $\alpha$  (TNF- $\alpha$ ), B: High Mobility Group Box 1 (HMGB1). Results are expressed as mean  $\pm$  SEM for six animals in each group. \*\*\*: significant difference from the related sham group at  $P < 0.001$ , \*\*: significant difference from CLP-Heart group at  $P < 0.001$ .

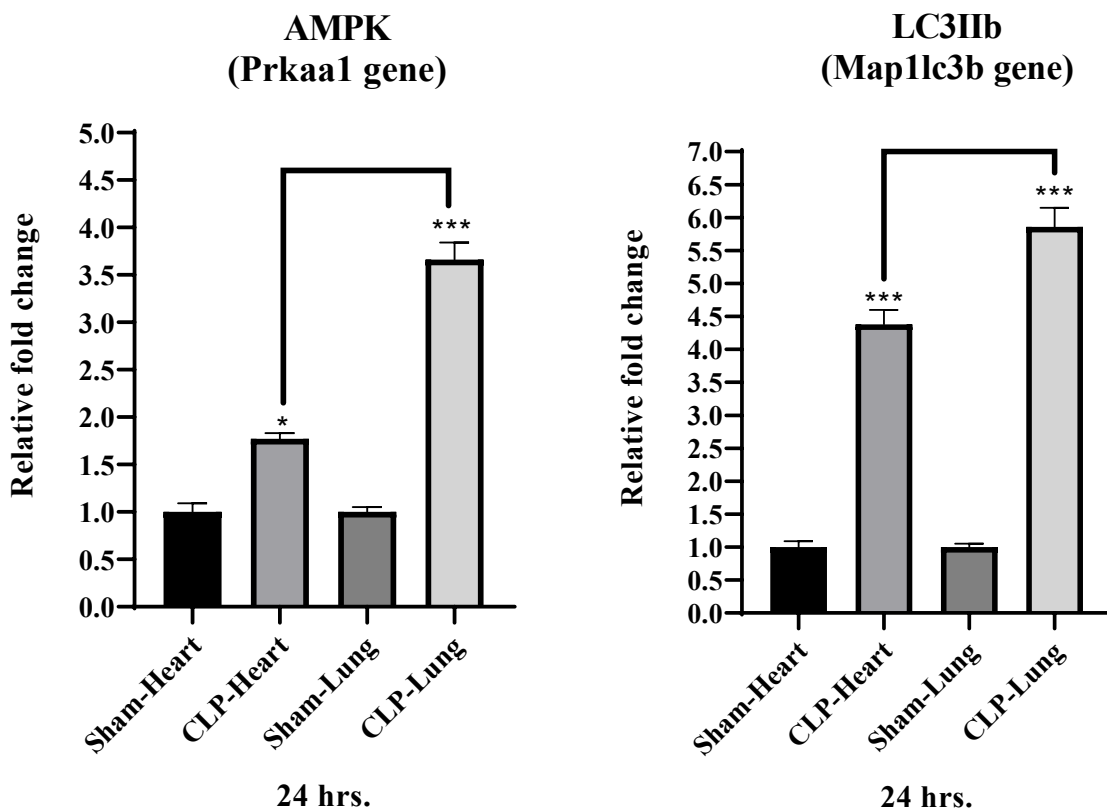


Fig. 2. The m-RNA gene expression level of Prkaa1 (AMPK related gene) and Map1lc3b (LC3IIb related gene) using RT-qPCR. Results are expressed as mean  $\pm$  SEM for six animals in each group. Samples were analyzed in triplicate. RT-qPCR (real-time reverse transcription-polymerase chain reaction); PRKAA1 (Protein Kinase AMP-Activated Catalytic Subunit Alpha 1); MAP1LC3B (Microtubule Associated Protein 1 Light Chain 3 Beta). \*\*\*: significant difference from the related sham group at  $P < 0.001$ , \*: significant difference from the related sham group at  $P < 0.05$ , \*\*: significant difference from CLP-Heart group at  $P < 0.001$ , \*: significant difference from CLP-Heart group at  $P < 0.05$ .

Table 2. **The abbreviations and primers of proteins used for real time RT-qPCR.**

Gene name	Gene symbol	Primer sequence (5'-3')
Glyceraldehyde-3-phosphate dehydrogenase	GAPDH	F: AGTCTACTGGCGTCTTCACC R: CCACGATGCCAAAGTTGTCA
AMP-activated catalytic subunit alpha 1 (AMPK)	Prkaa1	F: CCGTCTTATAGTTCAACCAT R: TTCGTTTATTCTCTCTGTT
Microtubule-associated protein 1 light chain 3 beta (LC3IIb)	Map1lc3b	F: CAGTGATTATAGAGCGATACA R: GCCTTCTAATTATCTTGATGAG

injury such as hyperplasia of pneumocyte-type A, peribronchiolar inflammation, and hyperemia compared to the sham group. The thickness of the alveolar septa significantly increased in comparison to the normal area. However, lung inflammation was verified by the presence of inflammatory cells (lymphocyte) and edema. Moreover, the histopathological evaluation of the heart sample in the CLP group showed myocardial cell necrosis (Fig. 3).

## Discussion

We designed the current study to illuminate differences in cardiac and pulmonary tissue damages following the CLP G-18 procedure in rats 24 hours after the procedure. To our best

knowledge, this is the first study which aimed to investigate the differences between pulmonary and cardiac dysregulation with G-18 CLP. This was carried out through assessment of cellular and molecular sepsis mechanisms such as oxidative stress, expression of homeostatic-autophagic related genes, proinflammatory cytokines, apoptosis and tissue perfusion in male Wistar rats. The findings of our study demonstrated that 24 hours after the CLP procedure, inflammatory markers, tissue lactate levels, proinflammatory cytokines, caspases, and gene expression of cellular homeostasis and autophagy in samples were more pronouncedly increased in the lung tissues. Moreover, the increase of the aforementioned factors was more highly elevated in the pulmonary tissue in with the heart specimen of the CLP group. This should be taken into consideration for the development and execution of related protocols to increase the accuracy of the results and avoid waste of resources.

Oxidative stress is a major indicator of sepsis induced by the CLP procedure. Oxidative stress pathways and ROS generation are consisted of several components such as increased LPO levels, alternated metabolic gene expression, and increased MPO levels during the procedure.<sup>17, 18</sup> In this regard, many consider MPO as a major indicator of the neutrophil infiltration process.<sup>18-23</sup> It is demonstrated that sepsis-induced by G-18 can elevate ROS levels in the liver, colon, and kidney 16–24 hours following the procedure.<sup>24-27</sup> Congruently, the findings of our study demonstrated that 24 hours after the CLP procedure, pulmonary tissue was impaired more intensely than cardiac tissue in CLP-G18.

Lactate level is generally considered as a reliable indicator of tissue hypoperfusion, hypoxia, and altered microcirculation

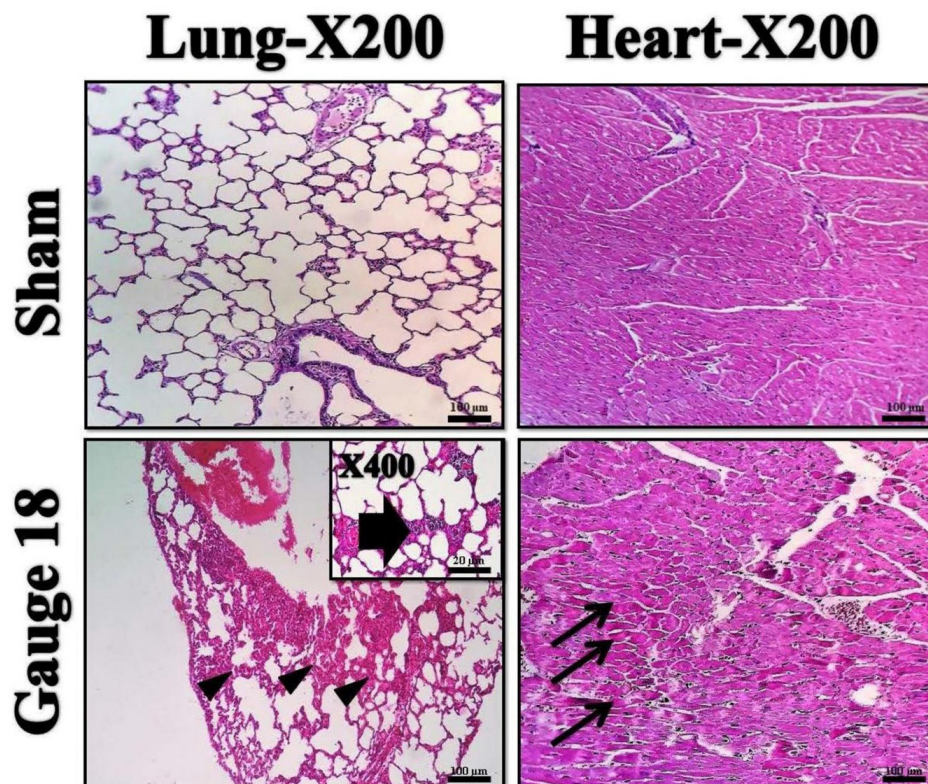


Fig. 3. **The histopathology of the lung and heart in sham and CLP groups.** Arrowheads: hyperplasia of pneumocyte type A, Thick arrow: perivascular inflammation and infiltration of inflammatory cells, Thin arrows: myocardial necrosis. 200 x (scale bar=100μm), 400 x (scale bar=20μm).

in CLP models of sepsis. Previous studies have separately reported raised lactate levels following CLP-G18 in blood, ileum, and liver, and noted the elevation of the lactate levels in the colon following CLP procedure with G22 needles.<sup>18, 20, 28-31</sup> In this regard, we observed that tissue lactate levels increased more intensely following CLP-G18 procedure in lung cells compared to heart tissue.

Regarding proinflammatory cytokines, it is demonstrated that the blood levels of these indicators of inflammation, particularly TNF- $\alpha$  and HMGB1, is altered during the CLP procedure.<sup>32-35</sup> Previous reports have demonstrated high levels of TNF- $\alpha$  in different organs of rats up to 72 hours after the CLP-G18 procedure.<sup>23, 24, 31, 36</sup> In this regard, we observed that in comparison with the cardiopulmonary system, the levels of both aforementioned cytokines were more intensely increased in pulmonary tissue compare to cardiac samples 24 hours after CLP-G18.

Mitochondrial membrane disturbance during ROS elevation results in activation caspases 9 and 3 with the natural consequence of cellular apoptosis.<sup>31</sup> This programmed cell death process during the CLP procedure is observed and reported in different tissues such as the kidney and brain.<sup>37, 38</sup> Correspondingly, findings of our study revealed that the levels of the aforementioned caspases increased in the lung more significantly in comparison of the heart in CLP-G18.

A combination of ROS elevation and enhanced autophagy is responsible for the elimination of abnormal proteins and the promotion of organ failure-related apoptosis during sepsis.<sup>39-43</sup> Several studies have demonstrated that the LC3-II/LC3-I ratio is increased in the liver, kidney, spleen, and mesenteric nodes after the CLP procedure.<sup>44-47</sup> Moreover, Hsiao et al showed an increase in LC3-II levels in the renal tissues of rat's 3 hours after CLP-G18. Correspondingly, Escobar concluded that 8 hours after the CLP-G22 procedure, LC3-II was increased in parallel with phosphorylated AMPK in the kidney and liver.<sup>39</sup> In this regard, we observed that the gene expression levels of mRNA of LC3-IIb and AMPK after CLP-G18 was more pronouncedly increased in the lung of the animals in comparison with the cardiac cells. Moreover, histopathological changes we observed confirmed the superiority of pulmonary impairment compared to cardiac cells in CLP-G18 in terms of provoking inflammation through demonstration of edematous and thickened lung tissues and myocardial cell necrosis. These observations support the hypothesis that in comparison with lung and heart organs 24 hours after CLP, pulmonary samples provoke oxidative stress reactions and cellular damage more pronouncedly compared to cardiac cells.

## Conclusion

In conclusion, findings of this study demonstrated that lung is superior to heart in terms of demonstration of the severity of sepsis induced in a rat model with CLP-G18, and both the rise of inflammatory markers and the extent of the ensuing organ damage is greater in the pulmonary cells undergone the procedure compared to cardiac cells with CLP G-18. It can be concluded that the choice of the tissue can have a great influence on the research outcomes, and this should be considered in the design and implementation of CLP studies so that researchers can cause the precise level of sepsis they intend to induce without waste of resources.

## Acknowledgments

This study was in part supported by a grant from TUMS coded 96-01-45-34820.

## Conflict of Interest

The authors declare that there is no known conflict of interest regarding this publication.

## References

- Drosatos K, Lymperopoulos A, Kennel PJ, Pollak N, Schulze PC, Goldberg IJ. Pathophysiology of sepsis-related cardiac dysfunction: driven by inflammation, energy mismanagement, or both? *Curr Heart Failure Repts*. 2015;12(2):130-40.
- Seymour CW, Gesten F, Prescott HC, Friedrich ME, Iwashyna TJ, Phillips GS, et al. Time to treatment and mortality during mandated emergency care for sepsis. *New Engl J Med*. 2017;376(23):2235-44.
- Sun Y, Cai Y, Zang QS. Cardiac autophagy in sepsis. *Cells*. 2019;8(2).
- Gonzalez MA, Ochoa CD. Multiorgan System Failure in Sepsis. *Sepsis*: Springer; 2018. p. 67-71.
- Park I, Kim M, Choe K, Song E, Seo H, Hwang Y, et al. Neutrophils disturb pulmonary microcirculation in sepsis-induced acute lung injury. *Eur Resp J*. 2019;53(3).
- Rittirsch D, Huber-Lang MS, Flierl MA, Ward PA. Immunodesign of experimental sepsis by cecal ligation and puncture. *Nat Protoc*. 2008;4(1):31.
- Dejager L, Pinheiro I, Dejonckheere E, Libert C. Cecal ligation and puncture: the gold standard model for polymicrobial sepsis? *Trends Microbiol*. 2011;19(4):198-208.
- Li L, Tan J, Miao Y, Lei P, Zhang Q. ROS and autophagy: Interactions and molecular regulatory mechanisms. *Cell Mol Neurobiol*. 2015;35(5):615-21.
- Aoki H, Kondo Y, Aldape K, Yamamoto A, Iwado E, Yokoyama T, et al. Monitoring autophagy in glioblastoma with antibody against isoform B of human microtubule-associated protein 1 light chain 3. *Autophagy*. 2008;4(4):467-75.
- Faubert B, Boily G, Izreig S, Griss T, Samborska B, Dong Z, et al. AMPK is a negative regulator of the Warburg effect and suppresses tumor growth in vivo. *Cell Metab*. 2013;17(1):113-24.
- Wichterman KA, Baue AE, Chaudry IH. Sepsis and septic shock--a review of laboratory models and a proposal. *J Surg Res*. 1980;29(2):189-201.
- Ebong S, Call D, Nemzek J, Bolgos G, Newcomb D, Remick D. Immunopathologic alterations in murine models of sepsis of increasing severity. *Infect Immun*. 1999;67(12):6603-10.
- Zapelini PH, Rezin GT, Cardoso MR, Ritter C, Klamt F, Moreira JC, et al. Antioxidant treatment reverses mitochondrial dysfunction in a sepsis animal model. *Mitochondrion*. 2008;8(3):211-8.
- Krawisz JE, Sharon P, Stenson WF. Quantitative assay for acute intestinal inflammation based on myeloperoxidase activity. Assessment of inflammation in rat and hamster models. *Gastroenterology*. 1984;87(6):1344-50.
- Rahimifard M, Navaei-Nigjeh M, Baeeri M, Maqbool F, Abdollahi M. Multiple protective mechanisms of alpha-lipoic acid in oxidation, apoptosis and inflammation against hydrogen peroxide induced toxicity in human lymphocytes. *Mol Cell Biochem*. 2015;403(1-2):179-86.
- Baeeri M, Momtaz S, Navaei-Nigjeh M, Niaz K, Rahimifard M, Ghasemi-Niri SF, et al. Molecular evidence on the protective effect of ellagic acid on phosalone-induced senescence in rat embryonic fibroblast cells. *Food Chem Toxicol*. 2017;100:8-23.
- Husain-Syed F, McCullough PA, Birk HW, Renker M, Brocca A, Seeger W, et al. Cardio-pulmonary-renal interactions: A multidisciplinary approach. *J Am Coll Cardiol*. 2015;65(22):2433-48.
- Goto M, Samonte V, Ravindranath T, Sayeed MM, Gamelli RL. Burn injury exacerbates hemodynamic and metabolic responses in rats with polymicrobial sepsis. *J Burn Care Res Off Publ Am Burn Assoc*. 2006;27(11):50-9.
- Liu H, Wu J, Yao JY, Wang H, Li ST. The role of oxidative stress in decreased acetylcholinesterase activity at the neuromuscular junction of the diaphragm during sepsis. *Oxidat Med Cell Longevity*. 2017;2017:1-6.
- Sener G, Sehirli O, Cetinel S, Ercan F, Yuksel M, Gedik N, et al. Amelioration of sepsis-induced hepatic and ileal injury in rats by the leukotriene receptor blocker montelukast. *Prostagl Leukotr Essent Fatty Acids*. 2005;73(6):453-62.

21. Sener G, Toklu H, Ercan F, Erkanli G. Protective effect of beta-glucan against oxidative organ injury in a rat model of sepsis. *Int Immunopharmacol*. 2005;5(9):1387-96.
22. Sener G, Toklu H, Kapucu C, Ercan F, Erkanli G, Kacmaz A, et al. Melatonin protects against oxidative organ injury in a rat model of sepsis. *Surg Today*. 2005;35(1):52-9.
23. Xiao X, Yang M, Sun D, Sun S. Curcumin protects against sepsis-induced acute lung injury in rats. *J Surg Res*. 2012;176(1):e31-9.
24. Chen HH, Lin KC, Wallace CG, Chen YT, Yang CC, Leu S, et al. Additional benefit of combined therapy with melatonin and apoptotic adipose-derived mesenchymal stem cell against sepsis-induced kidney injury. *J Pineal Res*. 2014;57(1):16-32.
25. Zhu W, Lu Q, Wan L, Feng J, Chen HW. Sodium tanshinone II A sulfonate ameliorates microcirculatory disturbance of small intestine by attenuating the production of reactive oxygen species in rats with sepsis. *Chin J Integr Med*. 2016;22(10):745-51.
26. Gonzalez AS, Elguero ME, Finocchietto P, Holod S, Romorini L, Miriuka SG, et al. Abnormal mitochondrial fusion-fission balance contributes to the progression of experimental sepsis. *Free Radic Res*. 2014;48(7):769-83.
27. Wang P, Huang J, Li Y, Chang R, Wu H, Lin J, et al. Exogenous carbon monoxide decreases sepsis-induced acute kidney injury and inhibits NLRP3 inflammasome activation in rats. *Int J Mol Sci*. 2015;16(9):20595-608.
28. Liaw WJ, Chen TH, Lai ZZ, Chen SJ, Chen A, Tzao C, et al. Effects of a membrane-permeable radical scavenger, Tempol, on intraperitoneal sepsis-induced organ injury in rats. *Shock*. 2005;23(1):88-96.
29. Tsao CM, Jhang JG, Chen SJ, Ka SM, Wu TC, Liaw WJ, et al. Adjuvant potential of selegiline in attenuating organ dysfunction in septic rats with peritonitis. *PLoS One*. 2014;9(9):1-9.
30. Yang S, Zhou M, Chaudry IH, Wang P. Novel approach to prevent the transition from the hyperdynamic phase to the hypodynamic phase of sepsis: role of adrenomedullin and adrenomedullin binding protein-1. *Ann Surg*. 2002;236(5):625-33.
31. Zhai X, Yang Z, Zheng G, Yu T, Wang P, Liu X, et al. Lactate as a potential biomarker of sepsis in a rat cecal ligation and puncture model. *Mediators Inflamm*. 2018;2018:1-9.
32. Abdulmahdi W, Patel D, Rabadi MM, Azar T, Jules E, Lipphardt M, et al. HMGB1 redox during sepsis. *Redox Biol*. 2017;13:600-7.
33. Léger T, Charrier A, Moreau C, Hinger-Favier I, Mourmoura E, Rigaudière JP, et al. Early sepsis does not stimulate reactive oxygen species production and does not reduce cardiac function despite an increased inflammation status. *Physiol Rep*. 2017;5(13):1-12.
34. Stevens NE, Chapman MJ, Fraser CK, Kuchel TR, Hayball JD, Diener KR. Therapeutic targeting of HMGB1 during experimental sepsis modulates the inflammatory cytokine profile to one associated with improved clinical outcomes. *Sci Rep*. 2017;7(1):1-14.
35. Lin WJ, Yeh WC. Implication of Toll-like receptor and tumor necrosis factor alpha signaling in septic shock. *Shock*. 2005;24(3):206-9.
36. Chang CL, Leu S, Sung HC, Zhen YY, Cho CL, Chen A, et al. Impact of apoptotic adipose-derived mesenchymal stem cells on attenuating organ damage and reducing mortality in rat sepsis syndrome induced by cecal puncture and ligation. *J Transl Med*. 2012;10:1-14.
37. Olguner CG, Koca U, Altekin E, Ergur BU, Duru S, Girgin P, et al. Ischemic preconditioning attenuates lipid peroxidation and apoptosis in the cecal ligation and puncture model of sepsis. *Exp Therap Med*. 2013;5(6):1581-8.
38. Zhou J, Chen Y, Huang GQ, Li J, Wu GM, Liu L, et al. Hydrogen-rich saline reverses oxidative stress, cognitive impairment, and mortality in rats submitted to sepsis by cecal ligation and puncture. *J Surg Res*. 2012;178(1):390-400.
39. Escobar DA, Botero-Quintero AM, Kautza BC, Luciano J, Loughran P, Darwiche S, et al. Adenosine monophosphate-activated protein kinase activation protects against sepsis-induced organ injury and inflammation. *J Surg Res*. 2015;194(1):262-72.
40. Nishida K, Kyoi S, Yamaguchi O, Sadoshima J, Otsu K. The role of autophagy in the heart. *Cell death Different*. 2009;16(1):31-8.
41. Zaha VG, Young LH. AMP-activated protein kinase regulation and biological actions in the heart. *Circul Res*. 2012;111(6):800-14.
42. Mizumura K, Cloonan S, Choi ME, Hashimoto S, Nakahira K, Ryter SW, et al. Autophagy: Friend or foe in lung disease? *Ann Am Thoracic Soc*. 2016;13(Supplement 1):S40-S7.
43. Mungai PT, Waypa GB, Jairaman A, Prakriya M, Dokic D, Ball MK, et al. Hypoxia triggers AMPK activation through reactive oxygen species-mediated activation of calcium release-activated calcium channels. *Mol Cell Biol*. 2011;31(17):3531-45.
44. Hsieh CH, Pai PY, Hsueh HW, Yuan SS, Hsieh YC. Complete induction of autophagy is essential for cardioprotection in sepsis. *Ann Surg*. 2011;253(6):1190-200.
45. Lee S, Lee SJ, Coronata AA, Fredenburgh LE, Chung SW, Perrella MA, et al. Carbon monoxide confers protection in sepsis by enhancing beclin 1-dependent autophagy and phagocytosis. *Antioxidants Redox Signal*. 2014;20(3):432-42.
46. Watanabe E, Muenzer JT, Hawkins WG, Davis CG, Dixon DJ, McDunn JE, et al. Sepsis induces extensive autophagic vacuolization in hepatocytes: a clinical and laboratory-based study. *Lab Invest J Techn Methods Pathol*. 2009;89(5):549-61.
47. Takahashi W, Hatano H, Hirasawa H, Oda S. Protective role of autophagy in mouse cecal ligation and puncture-induced sepsis model. *Critical Care*. 2013;17(2):1-13.

This work is licensed under a Creative Commons Attribution-NonCommercial 3.0 Unported License which allows users to read, copy, distribute and make derivative works for non-commercial purposes from the material, as long as the author of the original work is cited properly.